Inhibition of Human Acetyl- and Butyrylcholinesterase by Novel Carbamates of (−)- and (+)-Tetrahydrofurobenzofuran and Methanobenzodioxepine

Weiming Luo,[†,‡] Qian-sheng Yu,[†,‡] Santosh S. Kulkarni,[§] Damon A. Parrish,[||] Harold W. Holloway,[‡] David Tweedie,[‡] Avigdor Shafferman,[⊥] Debomoy K. Lahiri,[#] Arnold Brossi,[∞] and Nigel H. Greig*[,‡]

Drug Design & Development Section, Laboratory of Neurosciences, Gerontology Research Center, National Institute on Aging, National Institutes of Health, 5600 Nathan Shock Drive, Baltimore, Maryland 21224, Medicinal Chemistry Section, Intramural Research Program, National Institute on Drug Abuse, National Institutes of Health, 5500 Nathan Shock Drive, Baltimore, Maryland 21224, Laboratory for the Structure of Matter, Department of the Navy, Naval Research Laboratory, Washington, D.C. 20375, Department of Biochemistry and Molecular Genetics, Israel Institute for Biological Research, Ness-Ziona, 74100 Israel, Psychiatric Institute, Indiana University School of Medicine, Indianapolis, Indiana 46202, and School of Pharmacy, University of North Carolina at Chapel Hill, North Carolina 27599

Received June 17, 2005

A new enantiomeric synthesis utilizing classical resolution provided two novel series of optically active inhibitors of cholinesterase: (−)- and (+)-*O*-carbamoyl phenols of tetrahydrofurobenzofuran and methanobenzodioxepine. An additional two series of (−)- and (+)-*O*-carbamoyl phenols of pyrroloindole and furoindole were obtained by known procedures, and their anticholinesterase actions were similarly quantified against freshly prepared human acetyl- (AChE) and butyrylcholinesterase (BChE). Both enantiomeric forms of each series demonstrated potent cholinesterase inhibitory activity (with IC_{50} values as low as 10 nM for AChE and 3 nM for BChE), with the exception of the (+)-*O*-carbamoyl phenols of pyrroloindole, which lacked activity (IC_{50} values >1 μM). Based on the biological data of these four series, a structure−activity relationship (SAR) analysis was provided by molecular volume calculations. In addition, a probable transition-state model was established according to the known X-ray structure of a transition-state complex of *Torpedo californica* AChE−*m*-(*N*,*N*,*N*-trimethylammonio)-2,2,2-trifluoroacetophenone (*Tc*AChE−TMTFA). This model proved valuable in explaining the enantioselectivity and enzyme subtype selectivity of each series. These carbamates are more potent than, or similarly potent to, anticholinesterases in current clinical use, providing not only inhibitors of potential clinical relevance but also pharmacological tools to define drug−enzyme binding interactions within an enzyme crucial in the maintenance of cognition and numerous systemic physiological functions in health, aging, and disease.

Introduction

Dementia of the Alzheimer's type afflicts some 4.5 million Americans and some 18 million people worldwide. On the basis of the cholinergic hypothesis of memory, the depletion of its neurotransmitter acetylcholine (ACh), and loss of associated synapses during the progression of Alzheimer's disease (AD),[1,2] cholinesterase inhibitors (ChEIs) have been synthesized and developed for clinical practice to ameliorate the associated cognitive symptoms.[3] This is achieved by reducing the rate of hydrolysis of ACh in brain and thereby augmenting its cholinergic activity. Although ChEIs and the recently FDA approved drug memantine are the only ones to have consistently induced improvements in cognitive function in mild to moderate AD,[4] such improvements are, unfortunately, generally modest. Indeed, recent clinical trials have triggered debate as to the relevance of the benefit of this drug class.[5,6] Such concern has prompted two avenues of research: one to develop a new generation of ChEIs with activity beyond the modest symptomatic levels associated with initial agents, and another to optimize current agents on the basis of a greater understanding of enzyme/inhibitor interactions. Our research focus has been to undertake both simultaneously.

A classical ChEI, used to elucidate the original nature of chemical transmission of nerve action and the cholinergic system (Sir Henry Dale and Professor Otto Loewi, Nobel Prize 1936), is the natural product (−)-physostigmine (**15a**). An alkaloid isolated from the seeds of the Calabar bean, *Physostigma venenosum*,[7−9] (−)-physostigmine (**15a**) has provided a template in the development of several AD drugs, including rivastigmine (Novartis, Basel, Switzerland), phenserine (National Institute on Aging, Baltimore, MD, and Axonyx, New York, NY), eptylstigmine (Mediolanum, Milan, Italy), and the parent compound, itself, in a slow-release formulation (Synapton, Forrest Laboratories, St Louis, MO).[3,10,11] Extensive structure−activity relationship studies of this class of ChEIs indicate that (i) all derivatives of physostigmine with anticholinesterase activity are levorotary, with a 3a-*S* configuration in their pyrroloindole tricyclic ring system, and (ii) selectivity between the two cholinesterase forms, acetyl- (AChE, EC 3.1.1.7) and butyrylcholinesterase (BChE, EC 3.1.1.8), is primarily correlated with the structure of the N-substituted moiety of the carbamoyl side chain.[10−12]

An exception to the enantiomeric selectivity of physostigmine derivatives is the N^1-nor series of derivatives.[13,14] (−)-Physovenine (**20a**), a congeneric alkaloid of physostigmine,[9,10] also lacks enantiomeric selectivity.[10,15,16] The (+)-isomers of these two series of compounds, interestingly, have unexplainable anticholinesterase activity.[13−16] In our continuing effort to design new and improved ChEIs, we recently successfully synthesized

* To whom correspondence should be addressed: phone 410-558-8278; fax 410-558-8323; e-mail Greign@grc.nia.nih.gov.
† W.L. and Q.-S.Y. made equal contributions to this research and are equal first authors.
‡ National Institute on Aging, NIH.
§ National Institute on Drug Abuse, NIH.
|| Naval Research Laboratory.
⊥ Israel Institute for Biological Research.
Indiana University School of Medicine.
∞ University of North Carolina at Chapel Hill.

10.1021/jm050578p CCC: $33.50
Published on Web 03/11/2006

Scheme 1[a]

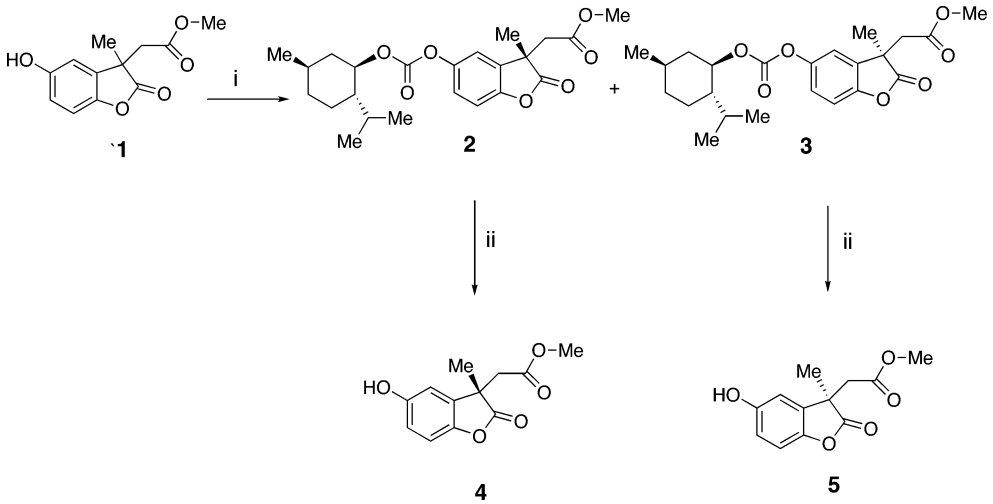

[a] (i) (a) (−)-Menthyl chloroformate, Et_3N, benzene, N_2, room temperature, 1.5 h; (b) recrystallized several times in hexane, then in ethanol. (ii) (a) NaOH, MeOH, room temperature, 1.5 h; (b) room temperature, 1 N HCl.

two novel series of bioactive racemic carbamates with the tricyclic skeletons furobenzofuran and methanobenzodioxepine.[17] Herein, we describe the synthesis and activity of their optically pure enantiomers with the dual purpose of (i) developing new AD drug candidates and (ii) utilizing them as tools to elucidate the molecular interactions required by the tricyclic skeleton of this important class of ChEI to achieve enantioselectivity within AChE and BChE.

Results

Chemistry. The starting material, 5-hydroxy-3-methyl-3-(methoxycarbonylmethylene)benzofuran-2-one (**1**), was produced from C3-alkylation of the condensation product of 1,4-cyclohexandione and pyruvic acid, according to a previously reported procedure.[17] First, compound **1** was reacted with (−)-menthyl chloroformate to provide a mixture of the stereoisomers of (3*S*)- and (3*R*)-menthyl carbonates of 5-hydroxy-3-methyl-3-(methoxycarbonylmethylene)benzofuran-2-one **2** and **3** (Scheme 1).

Since it proved difficult to isolate stereoisomers **2** and **3** with chromatography, we separated them by repeated crystallization. This was performed from hexane, at first, and then from ethanol to eventually yield two separate crystals with different crystalline forms: needle (**2**) and flaky (**3**) (Experimental Section).

The absolute configuration of the C-3 position was determined on the basis of the known configurations of C-19, C-21, and C-24 from compound **3** by X-ray crystallography. Figure 1 shows that compound **3** has an *R* configuration at its 3-position. As a consequence, compound **2** should possess an *S* configuration at its 3-position.

The use of chiral HPLC to measure the optical purity of compounds **2** and **3** proved unsuccessful. The hydrolysis of stereoisomers **2** and **3** provided (−)-enantiomer **4**, $[\alpha]_D^{26}$ −2.6° (c = 0.62, $CHCl_3$), and (+)-enantiomer **5,** $[\alpha]_D^{27}$ +2.2° (c = 0.45, $CHCl_3$) (Scheme 1), respectively. The enantiomeric excess value (ee, %) of each was measured by chiral HPLC analysis and is reported in the Experimental Section (Figure 2). Compounds **4** and **5** were, for practical purposes, optically pure. In the process of reduction, the stereochemistry at the 3-position of compounds **2** and **3** was unchanged. Hence, **2** gave **6a** (3a*S* configuration) and **7a** (5*S* configuration), whereas **3** gave **6b** (3a*R* configuration) and **7b** (5*R* configuration). The probable mechanism underpinning this reductive cyclization has recently

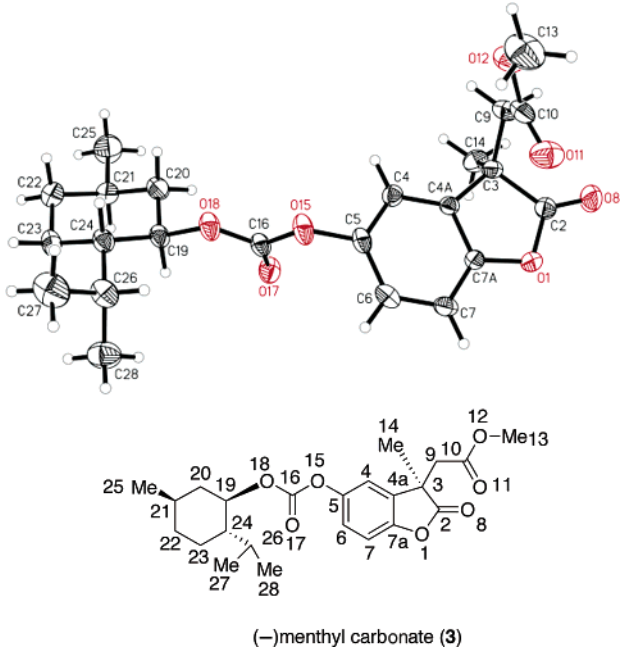

Figure 1. X-ray crystallographic picture and corresponding chemical structure of **3**.

been published.[17,18] In our recent prior research, we reported that the reductive cyclization of (±)-5-hydroxy-3-methyl-3-(methoxycarbonylmethylene)benzofuran-2-one by $LiAlH_4$ gave tetrahydrofurobenzofuran and methanobenzodioxipene in a yield of 10%.[17] In the present report, the reductive lithium−aluminum complexes of compound **2** and **3** were acidified by 1 M HCl in anhydrous Et_2O, instead of oxalic acid, to elevate the yield to approximately 30% (Scheme 2).

Phenols **6a** and **7a**, as well as **6b** and **7b**, were reacted with different isocyanates to give six pairs of corresponding carbamates: **8a** and **11a**, **9a** and **12a**, and **10a** and **13a**, as well as **8b** and **11b**, **9b** and **12b**, and **10b** and **13b**, respectively. Thereafter, each of these pairs of compounds was separated by preparative thin-layer chromatography (TLC), utilizing a procedure reported previously.[17]

The syntheses of carbamates of the physostigmine and physovenine series of analogues are shown in Scheme 3. Compounds **15a,b**, **17a**, **18a**, **20a,b**, **22a**, and **23a** are known compounds.[15,16] Compounds **16a** and **21a** were synthesized from

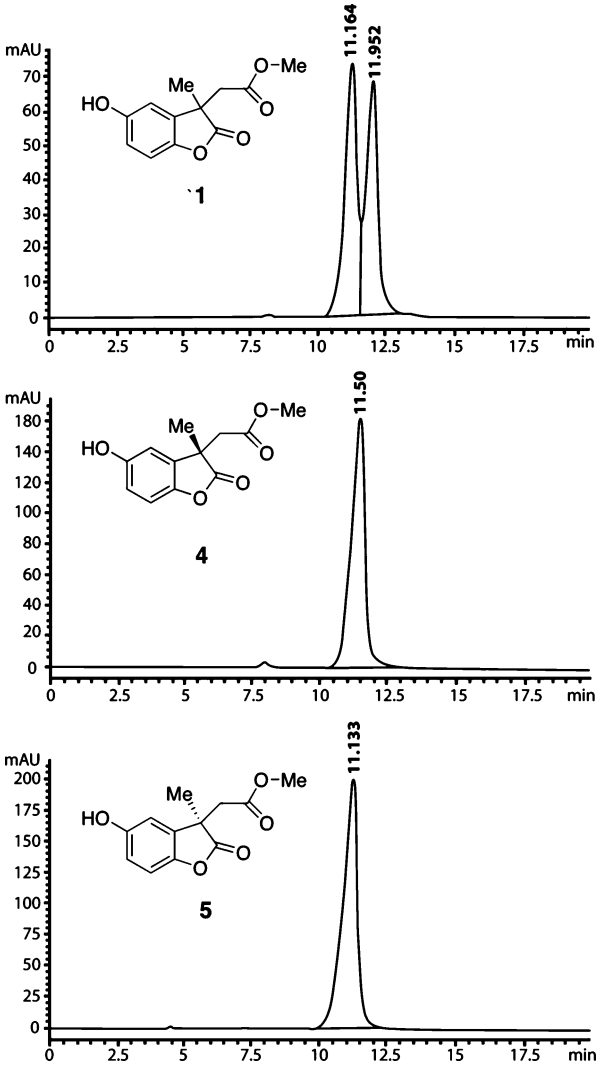

Figure 2. Chiral HPLC analysis of compounds **1**, **4**, and **5**. Instrument, HP1100; column, ChiraDex 5 μm; flow rate, 0.5 mL/min; detection, UV 254 nm; Eluent, MeOH/H_2O 45/55; temperature, room temperature. Retention times: **1**, 11.164 and 11.952 min; **4**, 11.50 min; **5**, 11.133 min.

compounds **14a** and **19a**, which were obtained from natural physostigmine according to a known procedure.[17] Compounds **17b**, **18b**, **22b**, and **23b** were synthesized from (+)-3a(*R*)-eseroline (**14b**) and (+)-3a(*R*)-physovenol (**19b**). These phenols, **14b** and **19b**, were obtained by asymmetric syntheses starting from *N*-methylphenetidine.[14]

X-ray Crystallography. The results of the X-ray studies of compound **3** are illustrated in Figure 1. The chirality of the asymmetric centers is as follows: C3-*R*, C19-*R*, C21-*R*, and C24-*S*. The six-membered ring of the menthyl moiety has a chair conformation; in contrast, the benzofuran system is flat.

Biological Evaluation. Table 1 shows the anticholinesterase activity of enantiomers **8**−**13**, **15**−**18**, and **20**−**23** against freshly prepared human AChE and BChE, derived from erythrocytes and plasma, respectively. The concentration of compound required to inhibit 50% enzyme activity (IC_{50} value) was quantified by a modified Ellman technique,[13−17,19−21] and values for *R*-configuration versus *S*-configuration are represented by the symbol *R*/*S*. A smaller IC_{50} is associated with a lower K_i value and a higher affinity of inhibitor−enzyme binding.[22−24] An *R*/*S* value of 1 is indicative of similar inhibitory activity for the *R*- and *S*-configurations. For an *R*/*S* value >1, the compound with *R*-configuration has a lower potency than its enantiomer.

Scheme 2[a]

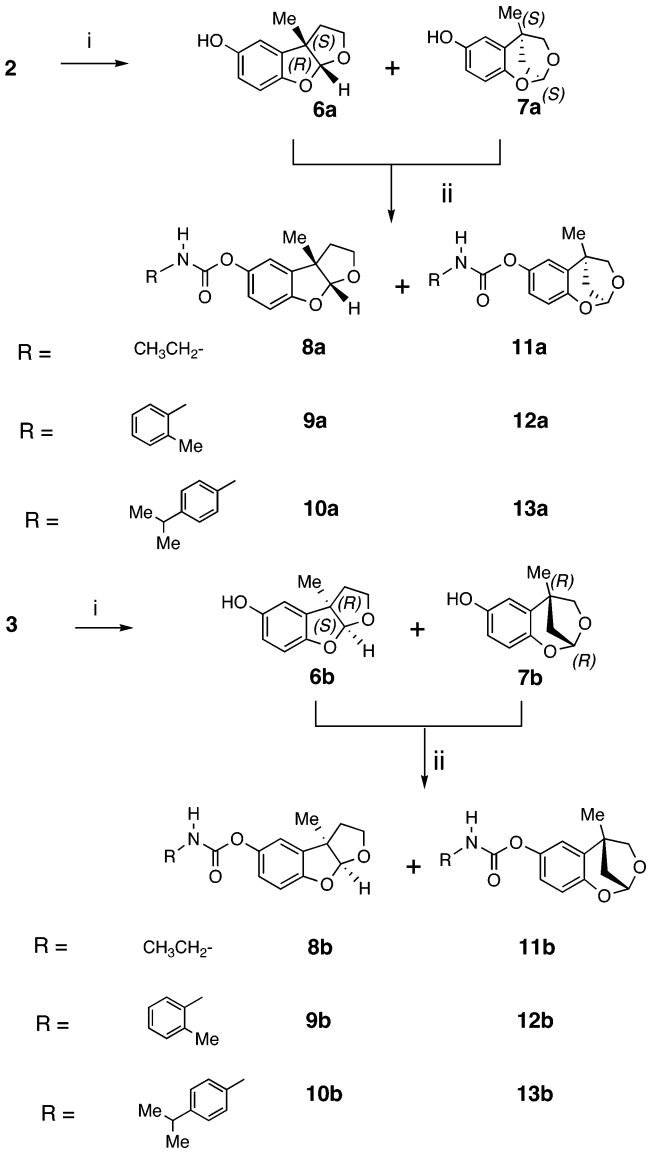

[a] (i) (a) LAH/Et_2O, room temperature, 1 h; (b) 1 M HCl in Et_2O, room temperature, 0.5 h. (ii) Na, RNCO/Et_2O, room temperature, 0.5−1.0 h.

With the sole exception of the compound pair **17a,17b**, which possessed low and approximately similar BChE inhibitory activity (*R*/*S* = 0.6), all compounds with a *S*-configuration proved to be more potent than their corresponding enantiomer (*R*/*S* > 1).

This was most evident in the physostigmine series, where AChE inhibitory activity was achieved with an *R*/*S* value ≥ 353 and BChE inhibitory action was achieved with an *R*/*S* value ≥ 102. Hence, in the physostigmine series, carbamates of (+)-physostigmine (**15b**, **17b**, and **18b**) possess minimal cholinergic activity, quite the opposite of their potent (−)-enantiomers.

In complete contrast with the physostigmine series, both enantiomers of the novel tetrahydrofurobenzofuran (**8a,b**, **9a,b**, and **10a,b**) and dihydrobenzodioxepine (**11a,b**, **12a,b**, and **13a,b**) series possessed potent anticholinesterase action for AChE, BChE, or both, with *R*/*S* values of ≤9.3. This activity is in accord with the congener physovenine carbamates (**20a,b**, **21a,b**, **22a,b**, and **23a,b**) that are similarly active in both enantiomeric forms with a preference for the *S*-configuration. As described, N-demethylation of physostigmine (**15a**) minimizes the enantioselectivity of this series,[14] which suggests that

Scheme 3[a]

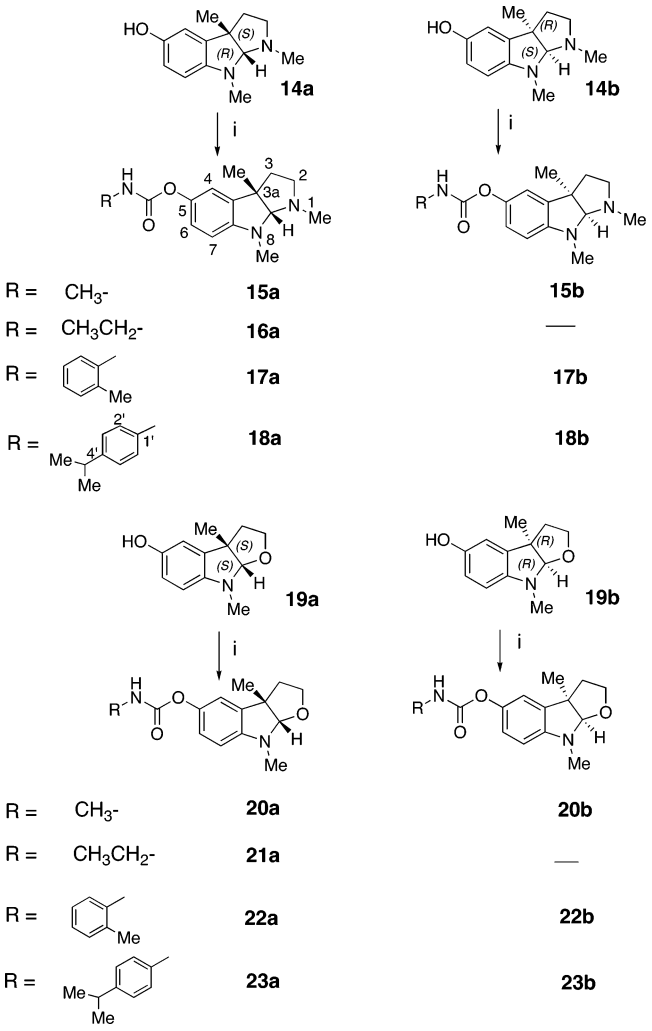

[a] (i) Na, RNCO/Et_2O, room temperature.

the N^1-substitution of the tricyclic ring is a key determinant regarding enantioselectivity. Additionally, the development of members of the tetrahydrofurobenzofuran and dihydrobenzodioxepine series for clinical development could be undertaken with either the potent *S*-(−)-enantiomers or the racemates, whose synthesis would be far easier and cheaper (avoiding optical resolution) and whose anticholinesterase activity is almost equal. A comparison of Tables 1 and 2, the latter defining the anticholinesterase activity of agents of current and recent clinical interest against enzyme drawn from the same individual and analyzed similarly, suggests that compounds **9a** and **12a** and compounds **10a** and **13a** possess sufficient potency and selectivity for AChE and BChE, respectively, to be of clinical interest.

In each of the four series of compounds detailed in Table 1, the differential selectivity for AChE or BChE is determined by the structure of N-substituted moiety of the carbamate. Specifically, the *N*-methylcarbamates provide minimal enzyme subtype selectivity. The *N*-ethylcarbamates have a moderate BChE preference. The *N*-2′-methylphenylcarbamates have high AChE selectivity, and *N*-4′-isopropylphenylcarbamates reverse this and demonstrate a high BChE preference. Of particular note, the AChE and BChE selectivities of the novel tetrahydrofurobenzofuran and dihydrobenzodioxepine series are among the greatest found of all ChEIs yet synthesized on the tricyclic backbone of physostigmine.

Discussion

Molecular Comparison by Volume Calculations. As all of the described carbamates possess close structural similarity as well as a similar inhibitory mechanism, we can initially compare them by means of superimposition to further elucidate the basis of their enantioselectivity. This was undertaken for the four AChE potent inhibitors with *S*-configuration (carbamates **9a**, **12a**, **17a**, and **22a**) by generating a molecular volume map′ of each molecule that corresponds to their van der Waals surface.[25,26]

As illustrated in Figure 3, for each compound, the relative positions of their two phenyl moieties, on either side of the carbonyl group in their optimized conformation, were almost identical, closely overlaying one another. These four compounds could be closely superimposed, except for disparity in their tricyclic systems. The combined molecular volume map of compounds **9a**, **12a**, **17a**, and **22a** provides an "enzyme-excluded map" (green area in Figure 3), within which all active compounds should fit.

The molecular volume of the *R*-2′-methylphenylcarbamates **9b**, **12b**, **17b**, and **22b** minus the enzyme-excluded volume provides an "estimate volume" that represents the additional volume generated by that of each *R*-isomer (yellow meshed area within Figure 3).

As shown in Table 3, the lowest estimate extra volume of compound **9b** (7.1 $Å^3$) corresponds to the lowest enantioselectivity ($R/S = 1.8$). The highest estimate extra volume (24.8 $Å^3$) of compound **17b** corresponds to the highest enantioselectivity ($R/S = 551$). Specifically, the larger estimate extra volume of compound **17b** (yellow meshed area in Figure 3) likely seriously hinders the approach to and hence binding between the inhibitor and enzyme. Molecular modeling studies were undertaken to elucidate how this additional estimate extra volume hinders binding.

Molecular Model of the Transition State. The wide structural diversity of available ChEIs suggests that unlike types of inhibitors bind with AChE in different ways via disparate yet specific interactions between compound and enzyme.[27−29] Most anticholinesterases, such as those in Table 2 as well as the potent nonclinical tacrine-based triazoles and other hybrids, are cationic at physiological pH, whereas some, including those of the present study and arisugacin, are not.[30−32] Human cholinesterases are large complex molecules composed of catalytic subunits that can clearly accommodate a variety of specific binding interactions associated with these diverse inhibitors. They contain up to 583 amino acids, have a molecular mass of 70−80 kDa, and are variably glycosylated.[29,33]

Three-dimensional analyses of AChE and BChE, based on X-ray crystallography, have provided structural information regarding the positioning of the catalytically important amino acid residues within these proteins.[34−41] In synopsis, three major binding domains have been described within AChE and two within BChE in an internalized, primarily hydrophobic gorge of some 20 Å length but as narrow as 0.5 Å wide. Deepest within this gorge is a catalytic acyl binding domain, which hydrolyzes choline esters through electron transfer within a catalytic triad, termed a charge relay system. The triad includes Ser_{200}, the imidazole group of His_{440}, and the carboxylic acid moiety of Glu_{327} (*Tc*AChE numbering). A choline binding domain resides midway along the gorge, and a peripheral anionic site exists at the gorge mouth for AChE but not BChE;[30−41] this latter site may be involved in the complexing of AChE with amyloid-β peptide in the Alzheimer brain.[42] Notably, the neurotoxicity associated with Aβ−AChE complexes has been

Table 1. 50% Inhibitory Concentrations of Compounds versus Freshly Prepared Human Erythrocyte AChE and Plasma BChE

no.	compounds	AChE (IC_{50}, nM, ± SEM)	*R*/*S*[a]	BChE (IC_{50}, nM, ± SEM)	*R*/*S*[a]	A/B[b]
		Carbamates of Tetrahydrofurobenzofuran				
8a	(−)-(3a*S*)-ethyl	100 ± 34		3 ± 1		33 BChE
8b	(+)-(3a*R*)-ethyl	486 ± 63	4.8	28 ± 1	9.3	17 BChE
9a	(−)-(3a*S*) -2′-methylphenyl	20 ± 1		11 400 ± 1300		570 AChE
9b	(+)-(3a*R*)-2′-methylphenyl	36 ± 1	1.8	36 400 ± 4750	3.2	1000 AChE
10a	(−)-(3a*S*)-4′-isopropylphenyl	c		13 ± 5		>2300 BChE
10b	(+)-(3a*R*)-4′-isopropylphenyl	6700 ± 1750		40 ± 2	3.1	167 BChE
		Carbamates of Benzodioxepine				
11a	(−)-(5*S*)-ethyl	610 ± 106		23 ± 5		27 BChE
11b	(+)-(5*R*)-ethyl	2420 ± 213	4.0	120 ± 66	5.3	20 BChE
12a	(+)-(5*S*) -2′-methylphenyl	38 ± 1.0		52 000 ± 10 000		1350 AChE
12b	(−)-(5*R*)-2′-methylphenyl	97 ± 4	2.6	c		>310 AChE
13a	(+)-(5*S*)-4′-isopropylphenyl	c		15 ± 1.5		>2000 BChE
13b	(−)-(5*R*)-4′-isopropylphenyl	3430 ± 145		54 ± 11	3.5	64 BChE
		Carbamates of Physostigmine[d]				
15a	(−)-(3a*S*)-methyl	28 ± 2		16 ± 3		2 BChE
15b	(+)-(3a*R*)-methyl	9890 ± 9	353	2490 ± 290	155	4 BChE
16a	(−)-(3a*S*)-ethyl[e]	94 ± 12		4 ± 1		24 BChE
17a	(−)-(3a*S*) -2′-methylphenyl	10 ± 2		1950 ± 240		195 AChE
17b	(+)-(3a*R*)-2′-methylphenyl	5510 ± 190	551	1180 ± 450	0.6	5 BChE
18a	(−)-(3a*S*)-4′-isopropylphenyl	760 ± 20		50 ± 1		15 BChE
18b	(+)-(3a*R*)-4′-isopropylphenyl	c		5100 ± 575	102	>6 BChE
		Carbamates of Physovenine[d]				
20a	(−)-(3a*S*)-methyl	27 ± 1		4 ± 1		7 BChE
20b	(+)-(3a*R*)-methyl	56 ± 1	2.1	56 ± 15	14	none
21a	(−)-(3a*S*)-ethyl[f]	82 ± 4		2 ± 0		40 BChE
22a	(−)-(3a*S*) -2′-methylphenyl	13 ± 1		1560 ± 120		120 AChE
22b	(+)-(3a*R*)-2′-methylphenyl	142 ± 135	11	5100 ± 1780	3.3	36 AChE
23a	(−)-(3a*S*)-4′-isopropylphenyl	3860 ± 970		17 ± 2		225 BChE
23b	(+)-(3a*R*)-4′-isopropylphenyl	c		23 ± 2	1.4	>1300 BChE

[a] IC_{50} of *R*-configuration/IC_{50} of *S*-configuration. [b] Selectivity for AChE or BChE from IC_{50} values. [c] None: Insufficient activity in the range of 0.3 nM−30 μM to calculate an IC_{50} value, and hence considered to be inactive. [d] The IC_{50} data for compounds **15a** and **15b** are from ref 14; the data for compounds **20a, 23a**, and **20b** are from ref 15; the data for compounds **17a, 22a**, and **18a** are from ref 16; and the data for compounds **16a** and **21a** are from ref 17. In each case, however, enzyme was obtained from the same individual and assays were performed similarly. [e] The (+)-(3a*R*)-ethylcarbamate compound was not synthesized. [f] The (+)-(3a*R*)-ethylcarbamate compound was not synthesized.

Table 2. Comparison of the IC_{50} Values (+ SEM) of Approved ChEIs of Clinical Interest versus Freshly Prepared Human Erythrocyte AChE and Plasma BChE (Figure 6)

compound	IC_{50} value[a] (nM ± SEM) AChE	BChE	selectivity
tacrine	190 ± 40	47 ± 10	4 BChE
donepezil	22 ± 8	4150 ± 1700	188 AChE
rivastigmine	4150 ± 160	37 ± 5	122 BChE
galanthamine	800 ± 60	7300 ± 830	9 AChE
(−)-phenserine	22 ± 1.4	1560 ± 45	70 AChE
(−)-(3a*S*)-Phenylcarbamate of Physostigmine			
heptylstigmine	22 ± 2	5.0 ± 0.1	4 BChE
(−)-(3a*S*)-Heptylcarbamate of Physostigmine			
huperzine A	47 ± 22	>10 000	>212 AChE
BW284c51[b]	18 ± 8	48 000	2660 AChE
iso-OMPA[b]	340 000	980 ± 550	350 BChE

[a] IC_{50} values were determined in duplicate on a minimum of four different occasions from enzyme collected from the same individual as assays described for Table 1. [b] BW284c51 [1,5-bis(4-allyldimethylammoniumphenyl)pentan-3-one dibromide] and iso-OMPA [tetra(monoisopropyl)pyrophosphortetramide] are classical selective inhibitors of AChE and BChE, respectively.

shown to be greater than that induced by the Aβ peptide alone in both cell culture and animal experiments.[39]

On the basis of calculations and electrooptical measurements, it has been suggested that electrostatic charges associated with seven negatively charged amino acids residues close to the entrance of the gorge trap and steer charged ligands into its mouth.[43,44] In the case of ACh, the quaternary choline moiety interacts with Trp_{84} of *Tc*AChE and, to a lesser extent, with Phe_{330} within the choline binding domain. This orientates the compound to allow the approach and nucleophilic attack of the catalytic triad on its carbonyl group. A quaternary transition state between Ser_{200} and ACh momentarily exists that then rapidly collapses into an acylated-enzyme intermediate and released choline. Thereafter, prompt hydrolysis of the acetyl ester reactivates the enzyme to allow efficient cleavage of as many as 10^4 ACh molecules s^{-1}.[37,38] (−)-Physostigmine (**15a**) and analogues interact similarly with the same two binding domains. However, nucleophilic attack of its carbonyl moiety results in a transient (−)-physostigmine−AChE intermediate, in a tetrahedral conformation, that then swiftly collapses to a carbamylated drug−enzyme complex that is dramatically more stable than the acetyl enzyme one associated with ACh; enzyme inhibition occurs consequent to the slow rate of enzyme decarbamylation. The inhibition process, hence, involves AChE-catalyzed hydrolyses of inhibitors.[37,38] In such a chemical reaction, the highest energy transition state controls the overall rate of the reaction. A catalytic enzyme can lower this energy barrier by specific interaction with the inhibitor in the transition state (**24**, **25**).[45] (Scheme 4). As shown in Table 1, each of the six different carbamates with the same N-substituted side chain (e.g., **8a,b**, **11a,b**, **16a**, and **21a**) should generate identical carbamylated enzyme structures after their reaction with either AChE or BChE. Hence their different IC_{50} values should be related to their affinities and rates of carbamylation, and not to decarbamylation, which would impact the time dependence of the inhibition associated with each. As a consequence, we can focus on carbamylation due to the short time frame of our biological studies.

A better insight into the molecular interactions of the enzyme and inhibitor can be obtained at the transition state. Whereas it is not currently possible to produce a crystal structure of an

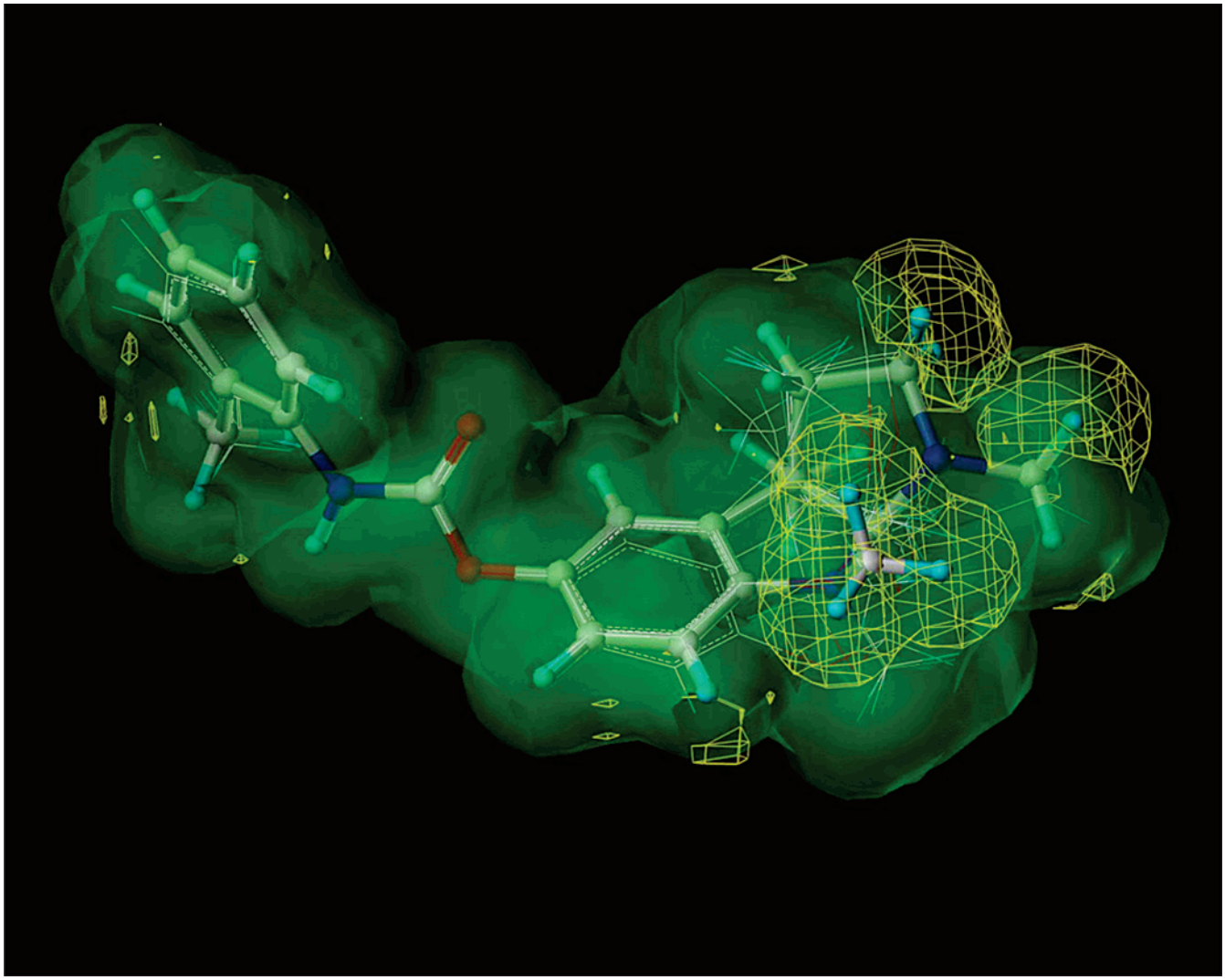

Figure 3. Union of molecular volume maps for the four active, *S*-configuration compounds **9a**, **12a**, **17a**, and **22a** (green area) provides the enzyme-excluded volume. The molecular volume map of compound **17b** minus the enzyme-excluded volume is the estimate extra volume of **17b** (yellow meshed area).

Table 3. Estimate Extra Volume[a] and the Ratio of Anticholinesterase Activity *R*/*S*

no.	compounds	estimate extra volume (Å^3)	*R*/*S* (AChE)
	Tetrahydrofurobenzofuran Series		
9b	(+)-(3a*R*)-2′-methylphenylcarbamate	7.1	1.8
	Dihydrobenzodioxepine Series		
12b	(−)-(5*R*)-2′-methylphenylcarbamate	19.9	2.6
	Physostigmine Series		
17b	(+)-(3a*R*)-2′-methylphenylcarbamate	24.8	551
	Physovenine Series		
22b	(+)-(3a*R*)-2′-methylphenylcarbamate	19.4	11

[a] Estimate extra volume = volume of *R*-configuration − enzyme-excluded volume map (union of volumes of active *S*-configuration compounds: **9a**, **12a**, **17a**, and **22a**).

enzyme complexed with its substrate in the transition state, due to the short transition-state lifetime versus the time required for X-ray data collection, one can exploit the high affinity of transition-state analogues. In this regard, the analogue *m*-(*N*,*N*,*N*-trimethylammonio)-2,2,2-trifluoroacetophenone (TMTFA), possessing a low K_i (15 fM) for inhibition of TcAChE,[46] was utilized to model the interaction of our compounds within the active site of AChE.

Scheme 4

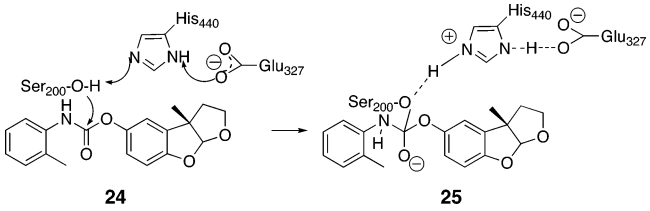

Prior investigation of the X-ray crystallographic structure of *Tc*AChE complexed with the known physostigmine analogue MF268 [8-(*cis*-2,6-dimethylmorpholino)octylcarbamoyleseroline] demonstrated the presence of a covalent bond between the carbonyl carbon and γ-O of Ser_{200} and also that the N-substituted side chain of the carbamoyl moiety is located inside the acyl-binding pocket and extends to the rim of the active site gorge.[47,48] The X-ray crystallographic transition-state analogue structure of *Tc*AChE−TMTFA (code 1AMN) was obtained from the RCSB protein databank. After extraction of TMTFA, the (−)-(3a*S*)-*N*-2′-methylphenylcarbamoyl phenol of furobenzofuran (**9a**) was docked, in accord with knowledge gained from the binding of MF268.[47,48]

As shown in Figure 4, six hydrogen bonds are apparent within the model (thin yellow lines): the NH of Gly_{118}, Gly_{119}, and

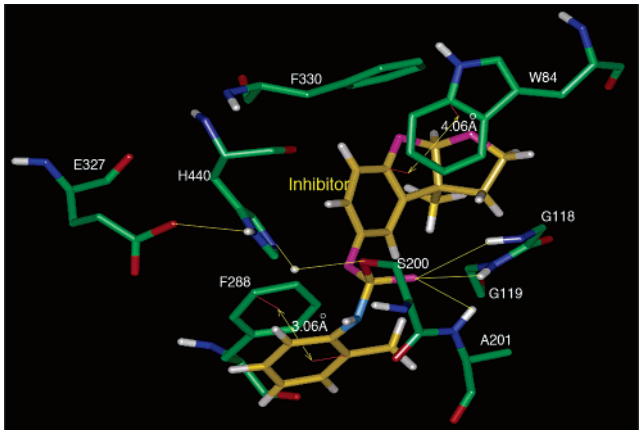

Figure 4. Close-up of compound **9a**−*Tc*AChE complex showing its covalent bonding with Ser_{200}. The thin yellow lines denote hydrogen bonds to the residues in the oxyanion hole, that is, Gly_{118}, Gly_{119}, and Ala_{201}, and in the catalytic triad, Ser_{200}, His_{440}, and Glu_{327}.

Ala_{201} with the oxygen of the ligand carbonyl, the γ-O of Ser_{200} with a single H, the hydrogen with N of His_{440}, and the NH of His_{440} with the oxygen of Glu_{327}. Together with the covalent bond of the γ-O of Ser_{200} with the C of the ligand's carbonyl group, the illustrated hydrogen bonds comprise an acylation site. This site is considered as a crucial part of the transition state. A transition state model was developed by (i) keeping the acylation site intact (by constraining the relative distances between the described atoms) and (ii) minimizing the complex energy, after automatic adjustment of the conformation of the remaining complex.

This model resembles a beam balance. The central supporting point is a covalent bond between the γ-O of Ser_{200} and the C of the ligand's carbonyl group. The $\pi-\pi$ interaction system between the N-phenyl group of carbamate (**9a**) and the phenyl group of Phe_{288} of the enzyme comprises one side of this balance. The $\pi-\pi$ or lipophilic (C−H$\cdots\pi$) interaction system of the furobenzofuran moiety of compound **9a** and the indole system of Trp_{84} of the enzyme forms the other side of the balance. Such C−H$\cdots\pi$ interactions have been observed in the X-ray crystal structure of other neutral molecules with *Tc*AChE.[49] Any change on either side of this balance may adversely affect the formation of the transition state. Utilizing this model, we can revisit the basis of enantioselectivity and enzyme subtype selectivity.

Enantioselectivity. As shown by molecular volume calculations (Figure 3, Table 3), for all carbamates with an *R*-configuration, with the exception of the physostigmine series, their molecular volumes are not greatly different. This would support the lipophilic interaction between the tricyclic ring system of the ligands and the indole system of Trp_{84} of the enzyme. Hence, all of these compounds retain substantial anticholinesterase activity compared to their *S*-isomers.

The only exception involves *R*-configuration compounds having an N^1-methyl group (the physostigmine series). The model predicts that the N^1-methyl group will become inserted between the tricyclic ring system and the indole system of Trp_{84}. The lipophilic interaction will consequently disappear, and a transition state between ligand and enzyme complex would not be readily formed without this lipophilic interaction. As a result, the (+)-physostigmine analogues **15b**, **17b**, and **18b** would be predicted to possess poor AChE and BChE inhibitory action, in accord with their measured poor ChEI activity.

Enzyme Subtype Selectivity. The acyl-binding pockets within AChE and BChE differ from one another in size and

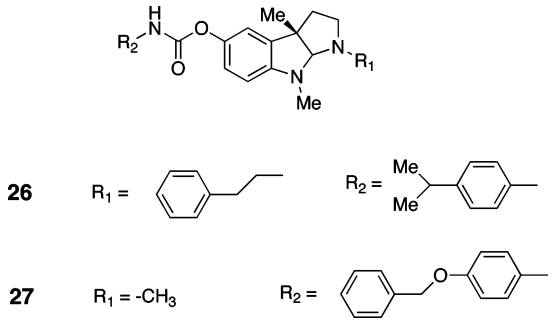

Figure 5.

shape. The pockets can be differentiated on the basis of two amino acid residues located at the bottom of the acyl loop. These residues are aromatic in AChE (Phe_{288} and Phe_{290}) but aliphatic in BChE (Leu_{286} and Val_{288}).[33,35,37,38,46] The latter pocket, hence, is slightly larger due to the smaller protruding side chains associated with Leu and Val.[12]

Our previous studies have shown that the conformational energy barrier of the *N*-phenyl group of compound **17a** and its analogues, rotated around the C1′−N bond, is correlated to the IC_{50} of AChE. A higher energy barrier is associated with a lower inhibitory activity (a larger IC_{50}); although, inexplicably, the energy barrier is as low as 0−0.7 kcal/mol. [21]

According to the described transition-state model (Figure 4), the $\pi-\pi$ interaction system between the *N*-phenyl group of the carbamate (**17a**) and the phenyl group of Phe_{288} of the enzyme comprises one side of this balance. Rotation of the *N*-phenyl group will decrease this $\pi-\pi$ interaction and directly influence the stability of the transition state, consequently lowering the affinity between ligand and enzyme.[21]

Utilizing the same model, we can now propose a basis for the cholinesterase subtype selectivity of the different carbamate moieties. (i) The small methyl group of *N*-methylcarbamates has almost no lipophilic interaction with residues of the acyl pocket; it thus has little influence on this balance and hence there is minimal subtype selectivity between AChE and BChE for *N*-methylcarbamates of all series. (ii) The ethyl group of *N*-ethylcarbamates, likewise, has relatively meager but nevertheless greater lipophilic interaction than *N*-methylcarbamates. The direction of this interaction is more favorable to form a stable transition state within BChE than AChE. Hence, all of the *N*-ethylcarbamates possess moderate BChE selectivity. (iii) The phenyl group of *N*-phenylcarbamates provides a significant lipophilic interaction with the aromatic ring of Phe_{288}. This interaction together with the lipophilic interaction between the tricyclic ring system and indole moiety of Trp_{84} provides a highly stable transition state. Thus, all *N*-phenyl- and *N*-methylphenylcarbamates possess potent AChE activity. Within BChE, however, Phe_{288} is replaced by an amino acid with an aliphatic residue. A similar $\pi-\pi$ interaction cannot be formed and leads to an unfavorable stability in the transition state and consequent weak BChE inhibitory activity. *N*-Phenyl- and *N*-methylphenylcarbamates hence have high AChE selectivity. Finally, (iv) the 4′-isopropylphenyl moiety of *N*-4′-isopropylphenylcarbamates cannot achieve a $\pi-\pi$ interaction within the acyl-binding pocket of AChE consequent to the bulk and hindering action of the isopropyl moiety. Within BChE, however, the lipophilic interaction of the isopropylphenyl group with residues of BChE in its larger acyl-binding pocket is favored (consequent to replacement of AChE Phe_{288} and Phe_{290} by Val and Leu), which stabilizes the transition state. Thus all of the *N*-4′-isopropylphenylcarbamate series have a potent and selective BChE inhibitory action.

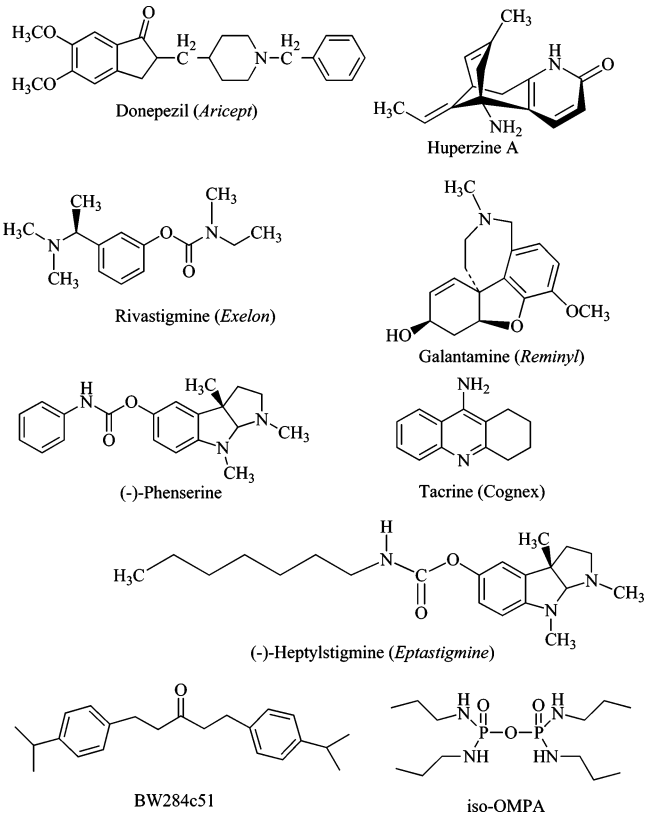

Figure 6. Chemical structures of clinically relevant cholinesterase inhibitors (Table 2).

In accord with this, one of the most potent and selective BChE inhibitors in the physostigmine series, (−)-N^1-phenethylnorcymserine (**26**) (IC_{50} for AChE >30 000 nM, IC_{50} for BChE 6.0 ± 1.0 nM, selectivity >5000-fold BChE) (Figure 5),[19] similarly can fit within the elongated acyl binding pocket associated with BChE. However, as the N^1-phenethyl moiety is directed outside the lipophilic interaction system, activity is not perturbed. Indeed, it is augmented, likely as a consequence of hydrophobic interactions close to the gorge mouth. Interestingly, the elongated (−)-4′-benzoxyphenylcarbamate of physostigmine, **27** (Figure 5),[50] which lacks a hindered 4′-isopropyl group, can maintain the $\pi-\pi$ interaction associated with potent AChE binding but make use of the larger acyl pocket associated with BChE to achieve BChE inhibitory potency (IC_{50} for AChE 58 ± 4 nM, IC_{50} for BChE 7.0 ± 1.0 nM, selectivity 7-fold BChE).[50]

In synopsis, we report a new enantiomeric synthesis, through classical resolution, of two novel series of potent anticholinesterases: the *O*-carbamoyl phenols of furobenzofuran and benzodioxepine. These two series provide candidates to selectively inhibit either AChE or BChE and, additionally, include some that possess neurotrophic actions.[17] Such actions may or may not be cholinergically mediated and provide this class of drugs actions beyond those that are classically considered to be only symptomatic.[51,52] Carbamates of these novel series are sufficiently active to be of potential clinical interest, comparing favorably with the inhibitory action of approved and recent ChEIs (Table 2, Figure 6), and could be developed either as their potent *S*-enantiomers or as their synthetically cheaper racemates. In addition, their enzyme subtype selectivity compares favorably with the classical selective anticholinesterases BW284c51 and iso-OMPA. On the basis of the described molecular volume calculations and known X-ray structure of a transition-state complex of *Tc*AChE−TMTFA, we have developed a beam balance-like transition-state model of the *Tc*AChE−*N*-phenylcarbamate complex. Using this model, we can now propose a basis to account for the enantioselectivity of physostigmine and its congeners.

Experimental Section

Chemistry. Melting points (uncorrected) were measured with a Fisher-Johns apparatus. ^{1}H NMR and ^{13}C NMR spectra were recorded on a Bruker (Bellevica, MA) AC-300 spectrometer. MS spectra (*m*/*z*) were recorded on a Hewlett-Packard 5973 gas chromatograph−mass spectrometer with chemical ionization [GC-MS (CI)]. High-resolution mass spectrometry (HRMS) was performed by the UCR Mass Spectrometry Facility, Department of Chemistry, University of California. Optical rotations were measured by Jasco, Model DIP-370 (Japan, Spectroscopic Co., Ltd.). Elemental analyses were performed by Atlantic Microlab, Inc. The ee % value of optically active compounds was determined by HPLC analyses using a HP1100 instrument and a chiral column (ChiraDex 5 μm) (Agilent Technology), mobile phase MeOH/H_2O = 45/55, elution rate 0.5 mL/min., UVD 254 nm, all at room temperature. All reactions involving nonaqueous solutions were performed under an inert atmosphere.

(3*S*)- and (3*R*)-Menthyl Carbonates of 5-Hydroxy-3-methyl-3-(methoxycarbonylmethylene)benzofuran-2-ones (2 and 3). Under a nitrogen atmosphere, a solution of 5-hydroxy-3-methyl-3-methoxycarbonylmethylenebenzofuran-2-one (**1**) (116 mg, 0.491 mmol) in 0.06 mL of triethylamine and 1.5 mL of benzene was dropwise added into (−)-menthyl chloroformate (118 mg, 0.539 mmol) at room temperature. The mixture was stirred for 1.5 h at the same temperature. The crude product was subjected to chromatography on silica gel (EtOAc/hexane = 1/3) to give 156.5 mg of white crystalline product, yield 76.2%: ^{1}H NMR ($CDCl_3$) δ 7.20−7.02 (m, 3H, Ar−H), 4.68−4.52 (m, 1H, CH−OC=O), 3.53 (s, 3H, CH_3O), 3.10, 2.96 (AB, J_{gem}=17.6 Hz, 2H, C3−CH_2COO), 2.21−2.11 (m, 1H, CH−^{i}Pr), 2.10−1.98 (m, 1H, CH−Me), 1.80−1.65 (m, 1H, $CHMe_2$), 1.51 (s, 3H, C3−CH_3), 1.59−1.41 (m, 2H, CH_2COC=O), 1.26−0.80 (m, 4H, CH_2CH_2), 0.97 (d, 6H, CH_3CCH_3) and 0.85 (d, 3H, CH_3CCCOC=O) ppm; CI-MS (CH_4), *m*/*z* 419 (MH^+), 418, 417, 371, 237, 181, 153 and 109; HR-MS *m*/*z* calcd for $C_{23}H_{34}NO_7$(MNH_4^+) 436.2335, found 436.2326. The above white crystal product was, thereafter, recrystallized from both hexane and ethanol, separately, several times, until the optical rotations and melting points of the two different isolated crystalline forms did not change. One, a needle crystalline form, was product **2**: mp 106.8−107.4 °C; $[\alpha]_D^{25}$ −60.8° (*c* = 0.53, $CHCl_3$). Anal. ($C_{23}H_{30}O_7$) C, H. The other, a flaky crystalline form, was product **3**: mp 148.0−148.8 °C; $[\alpha]_D^{26}$ −19.7° (*c* = 0.74, $CHCl_3$). Anal. ($C_{23}H_{30}O_7$) C, H.

(−)-(3*S*)-5-Hydroxy-3-methyl-3-(methoxycarbonylmethylene)-benzofuran-2-one (4). Under a nitrogen atmosphere, a mixture of reactant **2** (0.493 g, 1.178 mmol) and sodium hydroxide (0.2 g, 5.0 mmol) in 18 mL of methanol was stirred for 1.5 h at room temperature. It was then neutralized with 1 N HCl. After removal of solvent, the residue was chromatographed on silica gel (CH_2Cl_2/MeOH = 10/1) to give 168.2 mg of product **4**, yield 60.4%: mp 157.0−159.0 °C; $[\alpha]_D^{26}$ −2.6° (*c* = 0.62, $CHCl_3$); ee = 100% (HPLC); ^{1}H NMR ($CDCl_3$) δ 6.92−6.61 (m, 3H, Ar−H), 5.07 (s, 1H, OH), 3.44 (s, 3H, OCH_3), 3.02, 2.84 (AB, J_{gem} = 18.0 Hz, 2H, C3−CH_2C=O), and 1.41(s, 3H, C3−CH_3) ppm; CI-MS (CH_4) *m*/*z* 237(MH^+), 205, 177, and 163.

(+)-(3*R*)-5-Hydroxy-3-methyl-3-(methoxycarbonylmethylene)-benzofuran-2-one (5). Compound **5** was prepared as described above, yield 66.0%: mp 156.0−158.6 °C; $[\alpha]_D^{27}$ +2.2° (*c* = 0.45, $CHCl_3$); ee = 100%. The ^{1}H NMR and CI-MS (CH_4) are the same as that of compound **4**.

(3a*S*)-5-Hydroxy-3a-methyl-2,3,3a,8a-tetrahydrofuro[2,3-*b*]-benzofuran (6a) and (5*S*)-7-Hydroxy-5-methyl-4,5-dihydro-2,5-methano-1,3-benzodioxepine (7a). Under a nitrogen atmosphere, a solution of compound **2** (177 mg, 0.423 mmol) in 2 mL of ether was added dropwise to lithium aluminum hydride (32 mg, 0.843

mmol) in ether at 0 °C. The mixture, after beomg stirred at 0 °C for 0.5 h, was stirred for another 1 h at room temperature. Thereafter, 1 M HCl ether solution was to provide a mixture of pH 3−4, which then was stirred for 0.5 h at room temperature. Next, the mixture was filtered and the filtrate was concentrated. The residue was subjected to chromatography on silica gel (EtOAc/hexane = 1/3) to give 24.4 mg of a mixture of compounds **6a** and **7a**. The GC−CI-MS and ^{1}H NMR of this mixture were the same as that of the racemic[17] and showed an approximate 1:1 molar ratio of (3a*S*)-5-hydroxy-3a-methyl-2,3,3a,8a-tetrahydrofuro[2,3-*b*]benzofuran (**6a**) and (5S)-7-hydroxy-5-methyl-4,5-dihydro-2,5-methano-1,3-benzodioxepine (**7a**). The yields were 30%, and the compounds were directly used as starting material for the next reactions.

(3a*R*)-5-Hydroxy-3a-methyl-2,3,3a,8a-tetrahydrofuro[2,3-*b*]-benzofuran (6b) and (5*R*)-7-Hydroxy-5-methyl-4,5-dihydro-2,5-methano-1,3-benzodioxepine (7b). Compounds **6b** and **7b** were prepared from compound 3, according to the procedure described for compounds **6a** and **7a**.

(−)-(3a*S*)-3a-Methyl-2,3,3a,8a-tetrahydrofuro[2,3-*b*]benzofuran-5-yl *N*-Ethylcarbamate (8a) and (−)-(5*S*)-5-Methyl-4,5-dihydro-2,5-methano-1,3-benzodioxepin-7-yl *N*-Ethylcarbamate (11a). Under a nitrogen atmosphere, two small pieces of sodium (about 1 mg) were added into a solution of mixture of **6a** and **7a** (24.4 mg, 0.127 mmol) in 5 mL of anhydrous ether at room temperature. This mixture was then stirred for 2 min, and ethyl isocyanate (30.1 μL, 0.381 mmol) was next added to the reaction mixture in one portion. An hour into the reaction at room temperature, 1.4 mL of water was added and the ether layer was separated. After drying over sodium sulfate and filtering, the filtrate was evaporated to remove solvent. The residue was chromatographed on silica gel plate (EtOAc/hexane = 1/3) to afford products **8a** and **11a**. Product **8a** (11.6 mg, 69.7%): $[\alpha]_D^{26}$ −92.2° (*c* = 0.09, $CHCl_3$); ee = 100%; ^{1}H NMR ($CDCl_3$) δ 6.87−6.60 (m, 3H, Ar−H), 5.77 (s, 1H, C8a−H), 4.89 (br s, 1H, NH), 4.06−3.56 (m, 2H, C2−H), 3.23 (m, 2H, C5−CH_2NHCOO), 2.13−1.91 (m, 2H, C3−H), 1.47 (s, 3H, C3a-CH_3), and 1.14 (t, 3H, C5−CH_3CH_2-NHCOO) ppm; CI-MS (CH_4) *m*/*z* 264 (MH^+), 193, 175, and 72. Anal. ($C_{14}H_{17}NO_4$) N, H; C, calcd 63.87, found 63.14. Product **11a** (14.1 mg, 84.6%): $[\alpha]_D^{25}$ −10.0° (*c* = 0.12, $CHCl_3$), ee = 100%; ^{1}H NMR ($CDCl_3$) δ 6.82−6.67 (m, 3H, Ar−H), 5.69 (d, *J* = 1.80 Hz, 1H, C2−H), 4.88 (br s, 1H, C7−NHCOO), 4.17, 3.70 (AB, J_{gem} = 7.20 Hz, 2H, C4−H), 3.22 (m, 2H, C-7CH_2NHCOO), 2.19−1.19 (m, 2H, C10−H), 1.41 (s, 3H, C5−CH_3), and 1.16 (t, 3H, C7−CH_3CH_2NHCOO) ppm; CI-MS (CH_4) *m*/*z* 264 (MH^+), 246, 220, 193, 175, 149, and 72. Anal. ($C_{14}H_{17}NO_4$) C, H; N, calcd 5.32, found 4.91.

(+)-(3a*R*)-3a-Methyl-2,3,3a,8a-Tetrahydrofuro[2,3-*b*]benzofuran-5-yl *N*-Ethylcarbamate (8b) and (+)-(5*R*)-5-Methyl-4,5-dihydro-2,5-methano-1,3-benzodioxepin-7-yl *N*-Ethylcarbamate (11b). Under a nitrogen atmosphere, two small pieces of sodium (about 1 mg) were added into a solution of mixture of **6b** and **7b** (26 mg, 0.135 mmol) in 5 mL of anhydrous ether at room temperature. The mixture was stirred for 2 min, and thereafter, ethyl isocyanate (32.8 μL, 0.408 mmol) was added to the reaction mixture in one portion. The reaction was continued for an hour at room temperature, 4.0 mL of water was then added, and the ether layer was separated. After drying over sodium sulfate and filtering, the filtrate was evaporated to remove solvent. Thereafter, the residue was subjected to chromatography on a silica gel plate (EtOAc/hexane = 1/3) to afford products **8b** and **11b**. Product **8b** (14.8 mg, 83.1%): $[\alpha]_D^{26}$ +92.5° (*c* = 0.08, $CHCl_3$); ee = 100%; ^{1}H NMR ($CDCl_3$) δ 6.87−6.60 (m, 3H, Ar−H), 5.77 (s, 1H, C8a−H), 4.89 (br s, 1H, NH), 4.06−3.56 (m, 2H, C2−H), 3.23 (m, 2H, C5−CH_2NHCOO), 2.13−1.91 (m, 2H, C3−H), 1.47 (s, 3H, C3a-CH_3), and 1.14 (t, 3H, C5−CH_3CH_2NHCOO) ppm; CI-MS (CH_4) *m*/*z* 264 (MH^+), 193, 175, and 72. Anal. ($C_{14}H_{17}NO_4$) C, H; N, calcd.5.32, found 4.78. Product **11b** (10.4 mg, 58.4%): $[\alpha]_D^{26}$ +10.0° (*c* = 0.05, $CHCl_3$); ee = 100%. ^{1}H NMR ($CDCl_3$) δ 6.82−6.67 (m, 3H, Ar−H), 5.69 (d, *J* = 1.80 Hz, 1H, C2−H), 4.88 (br s, 1H, C7−NHCOO), 4.17, 3.70 (AB, J_{gem}=7.20 Hz, 2H, C4−H), 3.22 (m, 2H, C-7CH_2NHCOO), 2.19−1.19 (m, 2H, C10−H), 1.41 (s, 3H, C5−CH_3), and 1.16 (t, 3H, C7−CH_3CH_2NHCOO) ppm; CI-MS (CH_4) *m*/*z* 264 (MH^+), 246, 220, 193, 175, 149, and 72. Anal. ($C_{14}H_{17}NO_4$) C, H, N.

(−)-(3a*S*)-3a-Methyl-2,3,3a,8a-Tetrahydrofuro[2,3-*b*]benzofuran-5-yl *N*-(*o*-Tolyl)carbamate (9a) and (+)-(5*S*)-5-Methyl-4,5-dihydro-2,5-methano-1,3-benzodioxepin-7-yl *N*-(*o*-Tolyl)-carbamate (12a). Under a nitrogen atmosphere, two small pieces of sodium (about 1 mg) were added into a solution of mixture of **6a** and **7a** (27.9 mg, 0.145 mmol) in 5 mL of anhydrous ether at room temperature. The mixture was stirred for 2 min, and then *o*-tolyl isocyanate (18.9 μL, 0.149 mmol) was added to the mixture in one portion. The reaction was continued for 35 min at room temperature, 4 mL of water then was added, and the ether layer was separated. After drying over sodium sulfate and filtering, the filtrate was evaporated to remove solvent. The residue was chromatographed on a silica gel plate (EtOAc/hexane = 1/3) to afford products **9a** and **12a**. Product **9a** (15.6 mg, 66.1%): $[\alpha]_D^{27}$ --103.0° (*c* = 0.10, $CHCl_3$); ee = 100%; ^{1}H NMR ($CDCl_3$) δ 7.84 (br s, 1H, NH), 7.32−6.70 (m, 7H, Ar−H), 5.89 (s, 1H, C8a−H), 4.18−3.68 (m, 2H, C2−H), 2.39−2.05 (m, 2H, C3−H), 2.31 (s, 3H, Ar−CH_3), and 1.56 (s, 3H, C3a-CH_3) ppm; CI-MS (CH_4) *m*/*z* 326 (MH^+). Anal. ($C_{19}H_{19}NO_4$) H; calcd C 70.14, N 4.25; found C 69.18, N 3.71. Product **12a** (15.0 mg, 63.5%): $[\alpha]_D^{27}$ +30.4° (*c* = 0.135, $CHCl_3$), ee = 100%; ^{1}H NMR ($CDCl_3$) δ 7.87 (br s, 1H, C7−NHCOO), 7.33−6.70 (m, 7H, Ar−H), 5.79 (d, *J* = 1.80 Hz, 1H, C2−H), 4.22, 3.79 (AB, J_{gem} = 6.84 Hz, 2H, C4−H), 2.37−2.01 (m, 2H, C10−H), 2.31 (s, 3H, Ar−CH_3), and 1.51 (s, 3H, C5−CH_3) ppm; CI-MS (CH_4) *m*/*z* 326 (MH^+). Anal. ($C_{19}H_{19}NO_4$) C; H calcd 5.89, found 6.36; N calcd 4.31, found 3.57.

(+)-(3a*R*)-3a-Methyl-2,3,3a,8a-Tetrahydrofuro[2,3-*b*]benzofuran-5-yl *N*-(*o*-Tolyl)carbamate (9b) and (−)-(5*R*)-5-Methyl-4,5-dihydro-2,5-methano-1,3-benzodioxepin-7-yl *N*-(*o*-Tolyl)-carbamate (12b). Under a nitrogen atmosphere, two small pieces of sodium (about 1 mg) were added into a solution of mixture of **6b** and **7b** (18 mg, 0.09 mmol) in 5 mL of anhydrous ether at room temperature. The mixture was stirred for 2 min, and then *o*-tolyl isocyanate (18.3 μL, 0.145 mmol) was added in one portion. The reaction was continued for a further 35 min at room temperature, 4 mL of water then was added and the ether layer was separated. After drying over sodium sulfate and filtering, the filtrate was evaporated to remove solvent. The residue was chromatographed on silica gel plate (EtOAc/hexane = 1/3) to afford products **9b** and **12b**. Product **9b** (11.0 mg, 74.9%), $[\alpha]_D^{26}$ +104.2° (*c* = 0.095, $CHCl_3$); ee = 100%; ^{1}H NMR ($CDCl_3$) δ 7.84 (br s, 1H, NH), 7.32−6.70 (m, 7H, Ar−H), 5.89 (s, 1H, C8a−H), 4.18−3.68 (m, 2H, C2−H), 2.39−2.05 (m, 2H, C3−H), 2.31 (s, 3H, Ar−CH_3) and 1.56 (s, 3H, C3a-CH_3) ppm; CI-MS (CH_4) *m*/*z* 326 (MH^+). Anal. ($C_{19}H_{19}NO_4$) C, H; N, calcd 4.31, found 3.78. Product **12b** (9.5 mg, 64.4%), $[\alpha]_D^{27}$ −29.0° (*c* = 0.10, $CHCl_3$); ee = 100%; ^{1}H NMR ($CDCl_3$) δ 7.87 (br s, 1H, C7−NHCOO), 7.33−6.70 (m, 7H, Ar−H), 5.79 (d, *J* = 1.80 Hz, 1H, C2−H), 4.22, 3.79 (AB, J_{gem} = 6.84 Hz, 2H, C4−H), 2.37−2.01 (m, 2H, C10−H), 2.31 (s, 3H, Ar−CH_3) and 1.51 (s, 3H, C5−CH_3) ppm; CI-MS (CH_4) *m*/*z* 326 (MH^+). Anal. ($C_{19}H_{19}NO_4$) N; Calcd C 70.14, N 5.89; Found C 69.49, N 5.46.

(−)-(3a*S*)-3a-Methyl-2,3,3a,8a-Tetrahydrofuro[2,3-*b*]benzofuran-5-yl *N*-(*p*-Isopropylphenyl)carbamate (10a) and (+)-(5*S*)-5-Methyl-4,5-dihydro-2,5-methano-1,3-benzodioxepin-7-yl *N*-(*p*-Isopropylphenyl)carbamate (13a). Under a nitrogen atmosphere, two small pieces of sodium (about 1 mg) were added into a solution of mixture of **6a** and **7a** (16 mg, 0.083 mmol) in 5 mL of anhydrous ether at room temperature. The mixture was stirred for 2 min, and *p*-isopropylphenyl isocyanate (14 μL, 0.086 mmol) was added to the mixture of 6a and 7a in one portion. The reaction was continued for an additional 45 min at room temperature; thereafter, 4 mL of water was added and the ether layer separated. After drying over sodium sulfate and filtering, the filtrate was evaporated to remove solvent. The residue was chromatographed on silica gel plate (EtOAc/hexane = 1/3) to afford products **10a** and **13a**. Product **10a** (8 mg, 54.4%): $[\alpha]_D^{26}$ −91.4° (*c* = 0.35, $CHCl_3$); ee = 100%; ^{1}H NMR ($CDCl_3$) δ 7.31−6.71 (m, 8H, Ar−H, HNCOO), 5.80 (s,

1H, C8a−H), 4.09−3.59 (m, 2H, C2−H), 2.82 (septet, $J = 5.24$ Hz, 1H, $CHMe_2$), 2.19−1.96 (m, 2H, C3−H), 1.49 (s, 3H, C3a-CH_3), and 1.18 (d, $J = 5.24$ Hz, 6H, CH_3CCH_3) ppm; CI-MS (CH_4) *m/z* 354 (MH^+). Anal. ($C_{21}H_{23}NO_4$) H; alcd C 71.37, N 3.94; Found C 70.86, N 3.30. Product **13a** (9 mg, 61.2%): $[\alpha]_D^{26}$ +50.0° (c = 0.2, $CHCl_3$); ee = 100%; ^{1}H NMR ($CDCl_3$) δ 7.30−6.72 (m, 8H, Ar−H, HNCOO), 5.71 (d, $J = 1.80$ Hz, 1H, C2−H), 4.17, 3.70 (AB, $J_{gem} = 5.40$ Hz, 2H, C4−H), 2.81 (septet, $J = 5.22$ Hz, 1H, $CHMe_2$), 2.19−1.94 (m, 2H, C10−H), 1.48 (s, 3H, C5−CH_3), and 1.19 (d, $J = 5.22$ Hz, 6H, CH_3CCH_3) ppm; CI-MS (CH_4) *m/z* 354 (MH^+). Anal. ($C_{21}H_{23}NO_4$) C, H; N, calcd 3.96, found 4.56.

(+)-(3a*R*)-3a-Methyl-2,3,3a,8a-Tetrahydrofuro[2,3-*b*]benzofuran-5-yl *N*-(*p*-Isopropylphenyl)carbamate (10b) and (−)-(5*R*)-5-Methyl-4,5-dihydro-2,5-methano-1,3-benzodioxepin-7-yl *N*-(*p*-Isopropylphenyl)carbamate (13b). Under a nitrogen atmosphere, two small pieces of sodium (about 1 mg) were added into a solution of mixture of **6b** and **7b** (18 mg, 0.094 mmol) in 5 mL of anhydrous ether at room temperature. The mixture was stirred for 2 min, and then *p*-isopropylphenyl isocyanate (14.6 μL, 0.096 mmol) was added in one portion. The reaction was continued for a further 45 min at room temperature, and then 4 mL of water was added and the ether layer separated. After drying over sodium sulfate and filtering, the filtrate was evaporated to remove solvent. The residue was chromatographed on a silica gel plate (EtOAc/hexane = 1/3) to afford products **10b** and **13b**. Product **10b** (13.7 mg, 82.1%): $[\alpha]_D^{27}$ +91.4° (c = 0.14, $CHCl_3$); ee = 100%; ^{1}H NMR ($CDCl_3$) δ 7.31−6.71 (m, 8H, Ar−H, HNCOO), 5.80 (s, 1H, C8a−H), 4.09−3.59 (m, 2H, C2−H), 2.82 (septet, $J = 5.24$ Hz, 1H, $CHMe_2$), 2.19−1.96 (m, 2H, C3−H), 1.49 (s, 3H, C3a−CH_3), and 1.18 (d, $J = 5.24$ Hz, 6H, CH_3CCH_3) ppm; CI-MS (CH_4) *m/z* 354 (MH^+). Anal. ($C_{21}H_{23}NO_4 \cdot {}^1/_8H_2O$) C, H, N. Product **13b** (10.1 mg, 60.4%): $[\alpha]_D^{27}$ −48.0° (c = 0.1, $CHCl_3$); ee = 100%; ^{1}H NMR ($CDCl_3$) δ 7.30−6.72 (m, 8H, Ar−H, HNCOO), 5.72 (d, $J = 1.80$ Hz, 1H, C2−H), 4.17, 3.70 (AB, $J_{gem} = 5.40$ Hz, 2H, C4−H), 2.81 (septet, $J = 5.22$ Hz, 1H, $CHMe_2$), 2.19−1.94 (m, 2H, C10−H), 1.48 (s, 3H, C5−CH_3), and 1.19 (d, $J = 5.22$ Hz, 6H,CH_3CCH_3) ppm; CI-MS (CH_4) *m/z* 354 (MH^+). Anal. ($C_{21}H_{23}NO_4$) H, N; C, calcd 71.37, found 70.75.

(+)-(3a*R*)-1,3a,8-Trimethyl-1,2,3,3a,8,8a-hexahydropyrrolo-[2,3-*b*]indol-5-ol (14b). Compound **14b** was synthesized, according to the procedure for its enantiomer, from *N*-methylphenetidine.[14]

(+)-(3a*R*)-1,3a,8-Trimethyl-1,2,3,3a,8,8a-hexahydropyrrolo-[2,3-*b*]indol-5-yl *N*-(2′-Methylphenyl)carbamate (17b). Compound **17b** was made, according to the procedure for its antipode, from *o*-tolyl isocyanate and (+)-eseroline:[21] $[\alpha]_D^{26}$ +68.2° (c = 0.2, $CHCl_3$); ^{1}H NMR and MS were the same as reported for its enantiomer.[21] Anal. ($C_{21}H_{25}N_3O_2$) H; Calcd C 71.70, N 11.95; found C 70.08, N 11.45.

(+)-(3a*R*)-1,3a,8-Trimethyl-1,2,3,3a,8,8a-hexahydropyrrolo-[2,3-*b*]indol-5-yl *N*-(4′-Isopropylphenyl)carbamate (18b). Compound **18b** was synthesized, according to the procedure for its antipode, from *p*-isopropylphenyl isocyanate and (+)-eseroline:[21] $[\alpha]_D^{26}$ +67.5° (c = 0.2, $CHCl_3$); ^{1}H NMR and MS were the same as reported for its enantiomer.[21] Anal. ($C_{23}H_{29}N_3O_2$) H, N; C, calcd 72.79, found 71.70.

(+)-(3a*R*)-3a,8-Dimethyl-2,3,3a,8a-tetrahydrofuro[2,3-*b*]indol-5-ol (19b). Compound **19b was** made according to the procedure for synthesis of its enantiomer.[14,17]

(+)-(3a*R*)-3a,8-Dimethyl-2,3,3a,8a-tetrahydrofuro[2,3-*b*]indol-5-yl *N*-(2′-Methylphenyl)carbamate (22b). Compound **22b** was synthesized, according to the procedure for its antipode, from *o*-tolyl isocyanate and (+)-eseroline:[21] $[\alpha]_D^{26}$ +27.5° (c = 0.2, $CHCl_3$); ^{1}H NMR and MS were the same as reported for its enantiomer.[20] Anal. ($C_{20}H_{22}N_2O_3$) C, H; N, calcd 8.28, found 7.84.

(+)-(3a*R*)-3a,8-Dimethyl-2,3,3a,8a-tetrahydrofuro[2,3-b]indol-5-yl *N*-(4′-Isopropylphenyl)carbamate (23b). Compound **23b** was made, according to the procedure for its antipode, from *p*-isopropylphenyl isocyanate and (+)-eseroline:[16] $[\alpha]_D^{26}$ +32.0° (c = 0.2, $CHCl_3$); ^{1}H NMR and MS were the same as reported for its enantiomer.[17] Anal. ($C_{22}H_{26}N_2O_3$) C, H; N, calcd 7.64, found 7.13.

X-ray Crystallography. A clear colorless crystal of dimensions 0.30 × 0.23 × 0.12 mm^2 was mounted on glass fiber using a small amount of Epoxy. Data were collected on a Bruker three-circle platform diffractometer equipped with a SMART 6000 CCD detector. The crystals were irradiated by use of a rotating anode Cu Kα source (λ = 1.541 78) with incident beam Göbel mirrors. Data collection was performed and the unit cell was initially refined with SMART (version 5.625).[53a] Data reduction was performed with SAINT (version 6.36A)[53b] and XPREP (version 6.12).[53c] Corrections were applied for Lorentz, polarization, and absorption effects by use of SADABS (version 2.03).[53d] The structure was solved and refined with the aid of the programs in the SHELXTL-plus (version 6.10) system of programs.[53e] The full-matrix least-squares refinement on F^2 included atomic coordinates and anisotropic thermal parameters for all non-H atoms. The H atoms were included by use of a riding model. The absolute configuration of C3 was established by making reference to unchanging chiral centers (C19, C21, and C24) in the synthetic procedure, with a resulting Flack parameter of −0.3(2).[53f] The X-ray data of compound **3** also can be found at the Cambridge Crystallographic Data Center (CCDC), http://www.ccdc.cam.ac.uk/. The reference number of this crystal is 285734.

Quantitation of Anticholinesterase Activity. The action of enantiomers **8**−**13** and compounds **17b**, **18b**, **22b**, and **23b** to inhibit the ability of freshly prepared human AChE and BChE to enzymatically degrade their respective specific substrates, acetyl-(β-methyl)thiocholine and *s*-butyrylthiocholine (0.5 mmol/L) (Sigma Chemical Co., St. Louis, MO), was quantified.[13−17,19−21] Samples of AChE and BChE were derived from freshly collected human whole red blood cells and plasma, respectively. Compounds were dissolved in Tween 80/EtOH 3:1 (v/v; <150 μL total volume) and were diluted in 0.1 M Na_3PO_4 buffer (pH 8.0) in half-log concentrations to provide a final concentration range that spanned from 0.3 nM to 30 μM. Tween 80/EtOH was diluted to in excess of 1:5000. No inhibitory action on either AChE or BChE was detected in separate experiments where the ChEI activity of the known compound **15a** was quantified in excess and without Tween 80/EtOH.

For the preparation of BChE, freshly collected blood was centrifuged (10000*g*, 10 min, 4 °C) and plasma was removed and diluted 1:125 with 0.1 M Na_3PO_4 buffer (pH 7.4). Plasma was carefully checked to ensure an absence of hemolysis. For AChE preparation, erythrocytes were washed five times in isotonic saline, lysed in 9 volumes of 0.1 M Na_3PO_4 buffer (pH 7.4) containing 0.5% Triton-X (Sigma), and then were diluted with an additional 19 volumes of buffer to a final dilution of 1:200.

Analysis of anticholinesterase activity was undertaken by utilizing a 25 μL sample of each enzyme preparation, at their optimal working pH (8.0), in 0.1 M Na_3PO_4 buffer (0.75 mL total volume). Compounds were preincubated with enzymes (30 min at room temperature) and then were incubated with their respective substrates and with 5,5′-dithiobis(2-nitrobenzoic acid) (25 min, 37 °C). The substrate/enzyme interaction was immediately halted by the addition of excess enzyme inhibitor (physostigmine, 1×10^{-5} M) and production of a yellow thionitrobenzoate anion was then measured by spectrophotometry at 412 nm λ. To correct for nonspecific substrate hydrolysis, aliquots were coincubated under conditions of absolute enzyme inhibition [by the addition of 1×10^{-5} M physostigmine (**15a**)], and the associated alteration in absorbance was subtracted from that observed through the concentration range of each test compound. Each agent was analyzed on four separate occasions and assayed alongside physostigmine (**15a**), as a control and external standard whose activity we have previously reported.[13−17,19−21] The mean enzyme activity at each concentration of test compound was then expressed as a percent of the activity in the absence of compound. This was transformed into a logit format (where logit = ln (% activity/100 minus % activity)) and then was plotted as a function of its log concentration. Inhibitory activity was calculated as an IC_{50}, defined as the concentration of compound (nanomolar) required to inhibit 50% of enzymatic activity, which was determined from a correlation between log

concentration and logit activity. Only results obtained from correlation coefficients of $r^2 \geq -0.98$ were considered acceptable. Studies that did not obtain this threshold were repeated.

Computer-Aided Molecular Modeling. Computer-aided molecular modeling was undertaken by using Sybyl version 7.0 (Tripos Inc., St. Louis, MO). The numbering of the amino acid residues is based on that for *Tc*AChE. Molecular volume calculations were performed by using multiple volume comparison routine. The atomic coordinates of the transition state of *Tc*AChE were obtained from the protein data bank (PDB entry 1AMN)[38] and were used for transition-state studies. In undertaking this, (i) molecules of water were removed, (ii) the small molecule *m*-(*N*,*N*,*N*-trimethylammonio)-2,2,2-trifluoroacetophenone (TMTFA) was extracted, and (iii) the carbonyl carbon of TMTFA was retained in the tetrahedral conformation. (iv) The carbonyl carbon of the inhibitor, (−)-(3a*S*)-*N*-(2′-methylphenyl)carbamoyl phenol of furobenzofuran (**9a**), was modified into the tetrahedral conformation and then superimposed with that of TMTFA, keeping both phenyl groups on the same side and, as much as possible, in a superimposed conformation. Thereafter, compound **9a** was merged into the active domain of *Tc*AChE. The covalent bond between carbonyl carbon of compound **9a** and γ-O of Ser_{200} was created. To maintain the hydrogen bonds associated with acylation, the distances between the NH of Gly_{118}, Gly_{119}, Ala_{201} and oxygen of the ligand carbonyl, γ-O of Ser_{200} and a single H, the hydrogen and N of His_{440}, the NH of His_{440} and oxygen of Glu_{327} were constrained. All the residues outside a radius of 10 Å from the compound **9a** were aggregated. The energy of the enzyme−inhibitor complex was minimized with the conjugate gradient algorithm.

Acknowledgment. We are grateful to the Medicinal Chemistry Section, National Institute on Drug Abuse, NIH, for use of chemical characterization and molecular modeling equipment. The research was supported, in part, by the Intramural Research Program of the National Institute on Aging, NIH. W.L. and Q.-S.Y. are supported via the MedStar Research Institute, Baltimore, MD, and S.S.K. is supported through a National Institutes of Health Visiting Fellowship. D.L. is funded via NIH grants (AG18379 and AG 18884) and the Alzheimer's Association.

Supporting Information Available: X-ray crystallographic data for compound **3** in CIF format; chiral HPLC spectra of compounds **1**, **4**, and **5**; and elemental analysis data. This material is available free of charge via the Internet at http://pubs.acs.org.

References

(1) Drachman, D. A.; Leavitt, J. Human memory and the cholinergic system. A relationship to aging? *Arch. Neurol.* **1974**, *30*, 113−21.
(2) Small, D. H. Do acetylcholinesterase inhibitors boost synaptic scaling in Alzheimer's disease? *Trends Neurosci.* **2004**, *27*, 245−9.
(3) Lahiri, D. K.; Rogers, J. T.; Sambamurti, K.; Greig, N. H. Rationale for the development of cholinesterase inhibitors as anti-Alzheimer agents. *Curr. Pharm. Des.* **2004**, *10*, 3111−9.
(4) Cummings, J. L. Cholinesterase inhibitors: A new class of psychotropic compounds. *Am. J. Psychiatry* **2000**, *157*, 4−15.
(5) Courtney, C.; Farrell, D.; Gray, R.; Hills, R.; Lynch, L.; Sellwood, E.; Edwards, S.; Hardyman, W.; Raftery, J.; Crome, P.; Lendon, C.; Shaw, H.; Bentham, P. AD2000 Collaborative Group. Long-term donepezil treatment in 565 patients with Alzheimer's disease (AD2000): randomised double-blind trial. *Lancet* **2004**, *363* (9427), 2105−15.
(6) Lopez, O. L.; Becker, J. T.; Saxton, J.; Sweet, R. A.; Klunk, W.; DeKosky, S. T. Alteration of a clinically meaningful outcome in the natural history of Alzheimer's disease by cholinesterase inhibition. *J. Am. Geriatr. Soc.* **2005**, *53*, 83−7.
(7) Conworth, E. In *The Alkaloids*; Manskel, R. H. F., Ed.; Academic: New York, 1965; Vol. 8, pp 27−46.
(8) (a) Robinson, B. In *The Alkaloids*; Manskel, R. H. F., Ed.; Academic: New York, 1967; Vol. 10, pp 383−401. (b) Robinson, B. In *The Alkaloids*; Manskel, R. H. F., Ed.; Academic: New York, 1971; Vol. 13, pp 213−226.
(9) Brossi, A. Bioactive Alkaloids. 4. Results of Recent Investigations with Colchicine and Physostigmine. *J. Med. Chem.* **1990**, *33*, 2311−2319.
(10) Greig, N. H.; Pei, X. F.; Soncrant, T. T.; Ingram, D. K.; Brossi, A. Phenserine and Ring C Hetero-Analogues: Drug Candidates for Treatment of Alzheimer's Disease. *Med. Res. Rev.* **1995**, *15*, 3−31.
(11) Greig, N. H.; Sambamurti. K.; Yu, Q. S.; Brossi, A.; Bruinsma, G.; Lahiri, D. K. An overview of phenserine tartrate, a novel acetylcholinesterase inhibitor for the treatment of Alzheimer's disease. *Curr. Alzheimer Res.* **2005**, *2*, 281−291
(12) Greig, N. H.; Sambamurti, K.; Yu, Q. S.; Perry, T. A.; Holloway, H. W.; Haberman, F,; Brossi, A,; Ingram, D. K.; Lahiri, D. K. Butyrylcholinesterase: its selective inhibition and relevance to Alzheimer's disease. In *Butyrylcholinesterase: Its Function and Inhibition*; Giacobini, E., Ed.; Martin Dunitz Ltd.: London, 2003; pp 69−90.
(13) Pei, X. F.; Greig, N. H.; Bi, S.; Broosi, A.; Toome, V. Inhibition of Human Acetylcholinesterase by Unnatural (+)-(3a*R*)-*N*1-Norphysostigmine and Arylcarbamate Analogues. *Med. Chem. Res.* **1995**, *5*, 265−270.
(14) Yu, Q. S.; Luo, W.; Holloway, H. W.; Utsuki, T.; Perry, T. A.; Lahiri, D. K.; Greig, N. H.; Brossi, A. Racemic N^1-Norphenserine and Its Enantiomers: Unpredicted Inhibition of Human Acetyl- and Butylylcholinesterase and β-Amyloid Precursor Protein *in vitro*. *Heterocycles* **2003**, *619*, 529−539.
(15) Yu, Q. S.; Liu, C.; Brzostowska, M.; Chrisey, L.; Brossi, A.; Greig, N. H. Physovenines: Efficient Synthesis of (−)- and (+)-Physovenine and Synthesis of Carbamate Analogues of (−)-Physovenine. Anticholinesterase Activity and Analgesic Properties of Optically Active Physovenines. *Helv. Chim. Acta* **1991**, *74*, 761−766.
(16) Brzostowska, M.; He, X. S.; Greig, N. H.; Rapoport, S.; Brossi, A. Phenylcarbamates of (−)-Eceroline and (−)-Physovenol: Selective Inhibition of Acetyl and, or Butyrylcholinesterases by Phenylcarbamates. *Med. Chem. Res.* **1992**, *2*, 238−246.
(17) Luo, W.; Yu, Q. S.; Zhan, M.; Parrish, D.; Deschamps, J. R.; Kulkarrni, S. S.; Holloway, H. W.; Alley, G.M.; Lahiri, D. K.; Brossi, A.; Greig, N. H. Novel Acetylcholinesterase based on the Molecular Skeletons of Furobenzofuran and Methanobenzodioxepine. *J. Med. Chem.* **2005**, *48*, 986−994.
(18) Luo, W.; Yu, Q. S.; Holloway, H. W.; Parrish D. A.; Greig, N. G.; Brossi, A. Syntheses of Tetrahydrofurobenzofurans and Dihydromethanobenzodioxepines from 5-Hydroxy-3-methyl-3*H*-benzofuran-2-one. Rearrangement and Ring Expansion under Reductive Conditions on Treatment with Hydrides. *J. Org. Chem.* **2005**, *70*, 6171−6176.
(19) Yu, Q. S.; Holloway, H. W.; Utsuki, T.; Brossi, A.; Greig, N. H. Phenserine-based synthesis of novel selective inhibitors of butyrylcholinesterase for Alzheimer's disease. *J. Med. Chem.*, **1999**, *42*, 1855−1861.
(20) Yu, Q. S.; Zhu, X.; Holloway, H. W.; Whittaker, N. F.; Utsuki, T,; Brossi, A.; Greig, N. H. Anticholinesterase activity of compounds related to geneserine tautomers—*N*-oxides and 1,2-oxazines. *J. Med. Chem.* **2002**, *45*, 3684−3691.
(21) Yu, Q. S.; Holloway, H. W.; Flippen-Anderson, F.; Hoffman, B.; Brossi, A.; Greig, N. H. Methyl analogues of the experimental Alzheimer drug, phenserine: synthesis and structure/activity relationships for acetyl- and butyrylcholinesterase inhibitory action. *J. Med. Chem.* **2001**, *44*, 4062−4071.
(22) Kamal, M. A.; Greig, N. H.; Alhomida, A. S.; Al-Jafari, A. A. Human acetylcholinesterase inhibition kinetics of the experimental Alzheimer therapeutic, tolserine. *Biochem. Pharmacol.* **2000**, *60*, 561−570.
(23) Al-Jafari, A. A.; Kamal, M. A.; Alhomida, A. S.; Greig, N. H. Brain acetylcholinesterase inhibition kinetics of two experimental Alzheimer's disease drugs, phenserine and tolserine, in the rat. *J. Biochem. Mol. Biol. Biophys.* **2000**, *4*, 323−335.
(24) Kamal, M. A.; Al-Jafari, A. A.; Greig, N. H. A new, simple and economical approach to analyze the inhibition kinetics of the enzyme, acetylcholinesterase, by using the experimental Alzheimer drug, tolserine. *Emir. Med. J.* **2002**, *20*, 333−337.
(25) Marshall, G. R.; Barry, C. D. Functional Representation of Molecular Volume for Computer-Aided Drug Design. Abstracts from the American Crystallographic Association, Honolulu, HI, 1979.
(26) Sufrin, J. R.; Dunn, D. A.; Marshall, G. R. Steric Mapping of the L-Methionine Binding Site of ATP: L-Methionine S-Adenosyltransferase. *Mol. Pharmacol.* **1981**, *19*. 307−313.
(27) Brufani, M.; Filocamo, L. Rational design of cholinesterase inhibitors. In *Cholinesterases and Cholinesterase Inhibitors*; Giacobini, E., Ed.; Martin Dunitz Ltd.: London, 2000; pp 27−46.
(28) Reiner, E.; Radic, Z. Mechanism of action of cholinesterase inhibitors. In *Cholinesterases and Cholinesterase Inhibitors*; Giacobini, E., Ed.; Martin Dunitz Ltd.: London, 2000; pp 27103−119.
(29) Greenblatt, H. M.; Dvir, H.; Silman, I.; Sussman, J. L. Acetylcholinesterase: a multifaceted target for structure-based drug design of anticholinesterase agents for the treatment of Alzheimer's disease. *J. Mol. Neurosci.* **2003**, *20*, 369−83.

(30) Krasiski, A.; Radi, Z.; Manetsch, R.; Raushel, J.; Taylor, P.; Sharpless, K. B.; Kolb H. C. In Situ Selection of Lead Compounds by Click Chemistry: Target-Guided Optimization of Acetylcholinesterase Inhibitors *J. Am. Chem. Soc.* **2005**, *127*, 6686−6692.
(31) Muñoz-Ruiz, P.; Rubio, L.; García-Palomero, E.; Dorronsoro, I.; Monte-Millán, M.; Valenzuela, R.; Usán, P.; Austra, C.; Bartolini, M.; Andrisano, V.; Bidon-Chanal, A.; Orozco, M.; Luque, F. J.; Medina, M.; Martínez, A. Design, synthesis and biological evaluation of dual binding site acetylcholinesterase inhibitors: new disease modifying agents for Alzheimer's disease. *J. Med. Chem*. **2005**, *48*, 7223−7233.
(32) Otoguro, K.; Kuno, F.; Omura, S. Arisugacins, selective acetylcholinesterase inhibitors of microbial origin. *Pharmacol. Ther*. **1997**, *76*, 45−54.
(33) Soreq, H.; Seidman, S. Acetylcholinesterase—new roles for an old actor. *Nat. Rev. Neurosci*. **2001**, *2*, 294−302.
(34) Massoulie, J. Molecular forms and anchoring of acetylcholinesterase. In *Cholinesterases and Cholinesterase Inhibitors*; Giacobini, E., Ed.; Martin Dunitz Ltd.: London, 2000; pp 81−102.
(35) Soreq, H.; Gnatt, A.; Loewenstein, Y.; Neville, L. F. Excavations into the active-site gorge of cholinesterases. *Trends Biochem. Sci*. **1992**, *17*, 353−8.
(36) Dvir, H.; Wong, D. M.; Harel, M.; Barril, X.; Orozco, M.; Luque, F. J.; Munoz-Torrero, D.; Camps, P.; Rosenberry, T. L.; Silman, I.; Sussman, J. L. 3D structure of *Torpedo californica* acetylcholinesterase complexed with huprine X at 2.1 A resolution: kinetic and molecular dynamic correlates. *Biochemistry* **2002**, *41*, 2970−81.
(37) Silman, I.; Millard, C. B.; Ordentlich, A.; Greenblatt, H. M.; Harel, M.; Barak, D.; Shafferman, A.; Sussman, J. L. A preliminary comparison of structural models for catalytic intermediates of acetylcholinesterase. *Chem.-Biol. Interact*. **1999**, *119*−*120*, 43−52.
(38) Silman, I.; Harel, M.; Axelsen, P.; Raves, M.; Sussman, J. L. Three-dimensional structures of acetylcholinesterase and of its complexes with anticholinesterase agents. *Biochem. Soc. Trans*. **1994**, *22*, 745−9.
(39) Nachon, F.; Asojo, O, A.; Borgstahl, G. E. O.; Masson, P. and Lockridge, O. Role of waterin aging of human butylcholinesterase inhibited by echothiophate: the crystal structure suggest two alternative mechanisms of aging. *Biochemistry* **2005**, *44*, 1154. (PDB codes: 1XLW, 1XLV, 1XLU).
(40) Nicolet, Y.; Lockridg, O.; Masson, P.; Fontecilla-Camps, J. C.; Nachon, F. Crystal Structure of Human Butyrylcholinesterase and of its Complexes with Substrate and Products. *J. Biol. Chem.* 2003, *278*, 41141 (PDB codes 1PO1, 1POM, 1POP, and 1POQ).
(41) Nachon, F.; Nicolet, Y.; Viguié, N.; Masson, P.; Fontecilla-Camps, J. C.; Lockridg, O. Engineering of a monomeric and low-glycosylated form of human butyrylcholinrsterase: expression, purification, characterization and crystallization. *Eur. J. Biochem*. **2002**, *269*, 630.
(42) Inestrosa, N. C.; Sagal, J. P.; Colombres, M. Acetylcholinesterase interaction with Alzheimer amyloid beta. *Subcell. Biochem*. **2005**, *38*, 299−317.
(43) Porschke, D.; Creminon, C.; Cousin, X.; Bon. C.; Sussman, J. L.; Silman, I. Electrooptical measurements demonstrate a large permanent dipole moment associated with acetylcholinesterase. *Biophys J*. **1996**, *4*, 1603−8.
(44) Felder, C. E.; Botti, S. A.; Lifson, S.; Silman, I,; Sussman, J. L. External and internal electrostatic potentials of cholinesterase models. *J. Mol. Graphics Modell*. **1997**, *15*, 318−27 and 335−7.
(45) Schowen, R. L. In *Transition States of Biochemical Processes*; Gandour, R. D., Schowen, R. L., Eds.; Plenum: New York, 1978; pp 555−578.
(46) Harel, M.; Quinn, D. Q.; Nair, H. K.; Silman, I.; Sussman, J. L. The X-ray Structure of a Transition State Analogue Complex Reveals the Molecular Origins of the Catalytic Power and Substrate Specificity of Acetylcholinesterase. *J. Am. Chem. Soc*. **1996**, *118*, 2340−2346.
(47) Perola, E.; Cellai, L.; Lamba, D.; Filocamo, L.; Brufani, M. Long Chain Analogues of Physostigmine as Potential Drugs for Alzheimer's Disease: New Insights Into the Mechanism of Action in the Inhibition of Acetylcholinesterase. *Biochim. Biophys. Acta* **1997**, *1343*, 41.
(48) Bartolucci, C.; Perola, E.; Cellai, L.; Brufani, M.; Lamba, D. "Back Door" Opening Implied by the Crystal Structure of Carbamoylated Acetylcholinesterase. *Biochemistry* **1999**, *38*, 5714.
(49) Koellner, G.; Steiner, T.; Millard, C. B.; Silman, I.; Sussuman, J. L. A Neutral Molecule in Cation-binding Site: Specific Binding of a PEG-SH to Acetylcholinesterase from *Torpedo californica*. *J. Mol. Biol*. **2002**, *320*, 721−725.
(50) Yu, Q. S.; Greig, N. H.; Holloway, H. W.; Brossi, A. 4′-Hydroxyphenylcarbamates of (3a*S*)-eseroline and (3a*S*)-*N*(1)-noreseroline: potential metabolites of the Alzheimer's anticholinesterase drug phenserine. *Heterocycles* **1999**, *50*, 95−102.
(51) Francis, P. T.; Nordberg, A.; Arnold, S. E. A preclinical view of cholinesterase inhibitors in neuroprotection: do they provide more than symptomatic benefits in Alzheimer's disease? *Trends Pharmacol. Sci.* **2005**, *26*, 104−11.
(52) Hashimoto, M.; Kazui, H.; Matsumoto, K.; Nakano, Y.; Yasuda, M.; Mori, E. Does donepezil treatment slow the progression of hippocampal atrophy in patients with Alzheimer's disease? *Am. J. Psychiatry* **2005**, *162*, 676−82.
(53) (a) SMART version 5.625; Bruker AXS Inc.: Madison, WI, 2001. (b) SAINT version 6.36A; Bruker AXS Inc.: Madison, WI, 2002. (c) XPREP version 6.12; Bruker AXS Inc.: Madison, WI, 2001. (d) SADABS version 2.03; Bruker AXS Inc.: Madison, WI, 2000. (e) SHELXTL version 6.10; Bruker AXS Inc.: Madison, WI, 2000. (f) Flack, H. D. *Acta Crystallogr*. **1983**, *A39*, 876−881.

JM050578P